Thermodynamics and superradiant phase transitions in a three-level Dicke model

Mathias Hayn and Tobias Brandes
Institut für Theoretische Physik, Technische Universität Berlin, 10623 Berlin, Germany
(Received 27 October 2016; published 27 January 2017)

We analyze the thermodynamic properties of a generalized Dicke model, i.e., a collection of three-level systems interacting with two bosonic modes. We show that at finite temperatures the system undergoes first-order phase transitions only, which is in contrast to the zero-temperature case where a second-order phase transition exists as well. We discuss the free energy and prominent expectation values. The limit of vanishing temperature is discussed as well.

DOI: 10.1103/PhysRevE.95.012153

I. INTRODUCTION

The Dicke superradiance model [1] as a test-bed for mean-field-like phase transitions [2] has received renewed attention recently, in particular due to its successful implementation in cold-atom experiments [3–7] and optical setups of cavities and lasers [8,9]. Much progress has been made toward a realistic description of nonequilibrium and dissipation [10–19], multimode effects [20], the interplay of the superradiant phase transitions and Bose-Einstein Condensation [21], spin glasses [22], the analysis of interactions [23], inhomogeneous couplings [24,25], finite-size effects [26], or the adiabatic limit [27,28]. Further extensions of the model have appeared allowing for driving [29,30], the creation of Goldstone modes [31–33], feedback control [34,35], or the transfer to other platforms such as solid-state systems [36,37].

In its simplest version, the Dicke model hosts a mean-field-type ground-state phase transition ("quantum bifurcation") at zero temperature [2,38,39] between a field-free (normal) phase with unpolarized atoms and a superradiant phase with macroscopic occupation of the field mode and polarization of the atoms. Above a critical coupling strength, the superradiant phase also persists at finite temperatures below a critical temperature, which defines the corresponding thermal second-order phase transition [40–43].

Thermal aspects of the Dicke-Hepp-Lieb superradiance phase transition have found recent interest again in the analysis of thermodynamic aspects like work extraction [44,45], and the discussion of van Hove-type singularities in the microcanonical density of states at large excitation energies [31,46–54] (excited state quantum phase transitions). This is our motivation to extend our previous studies [55,56] of an extended Dicke model toward finite temperatures in this paper.

In the original Dicke model [1], the atoms are approximated by two-level systems and the light field by a single (bosonic) mode of a resonator. Naturally, the questions arises what happens to the phases and phase transitions when the Dicke model is generalized by having more than just two (atomic) energy levels and one bosonic mode. In our previous study at zero temperature, we found an additional superradiant phase as well as phase transitions of first and second order in a three-level Dicke model interacting with two bosonic modes in Lambda configuration. These findings were also of interest in the context of the discussion of the no-go theorem [57–62] for superradiant phase transitions in this and other generalized Dicke models [36,56,63–66].

Our paper is organized as follows: first, we give a short review of the model and previous findings for zero temperature [55]. Then, the partition sum of the model is calculated in the thermodynamic limit from which we identify the thermodynamic phases relevant expectation values. We discuss the properties of the phases and the phase transitions and finally recover the zero-temperature results as a limiting case of our theory.

II. FINITE-TEMPERATURE PHASE TRANSITION IN THE Λ MODEL

A. The model

We consider a system of $\mathcal{N}$ three-level systems (the *particles*) in Λ configuration (cf. Fig. 1): two ground states $|1\rangle$, $|2\rangle$ with energies E_1, E_2, respectively, are coupled via two bosonic modes to the excited state $|3\rangle$ with energy E_3. The two bosonic modes have frequencies ω_1, ω_2, respectively. The Hamiltonian is given by (cf. Ref. [55])

$$\begin{aligned}\hat{H} &= \delta \hat{A}_2^{\,2} + \Delta \hat{A}_3^{\,3} + \hbar\omega_1 \hat{a}_1^\dagger \hat{a}_1 + \hbar\omega_2 \hat{a}_2^\dagger \hat{a}_2 \\ &\quad + \frac{g_1}{\sqrt{\mathcal{N}}}(\hat{a}_1^\dagger + \hat{a}_1)\left(\hat{A}_1^{\,3} + \hat{A}_3^{\,1}\right) \\ &\quad + \frac{g_2}{\sqrt{\mathcal{N}}}(\hat{a}_2^\dagger + \hat{a}_2)\left(\hat{A}_2^{\,3} + \hat{A}_3^{\,2}\right). \end{aligned} \tag{1}$$

Here, $\delta = E_2 - E_1$, $\Delta = E_3 - E_1$ and g_n is the coupling strength of nth bosonic mode. The operators $\hat{A}_n^{\,m}$,$n,m \in \{1,2,3\}$ are collective particle operators and can be written in terms of single-particle operators $\hat{a}_{n,m}^{(k)}$,

$$\hat{A}_n^{\,m} = \sum_{k=1}^{\mathcal{N}} \hat{a}_{n,m}^{(k)}. \tag{2}$$

The operator $\hat{a}_{n,m}^{(k)}$ acts on the degrees of freedom of the kth particle only and can be represented by $\hat{a}_{n,m}^{(k)} = |n\rangle^{(k)} \langle m|$, where $|n\rangle^{(k)}$ is the nth state of the kth three-level system.

We call the single-particle energy levels $|1\rangle$ ($|2\rangle$) and $|3\rangle$ together with the first (second) bosonic mode, the left (right) branch of the Λ model.

In a previous work [55], we have studied the ground-state properties of the Hamiltonian, Eq. (1), as well as collective excitations above the ground state. The model shows three phases: a normal phase and two superradiant phases. Both types of phases show their distinctive features as in the original

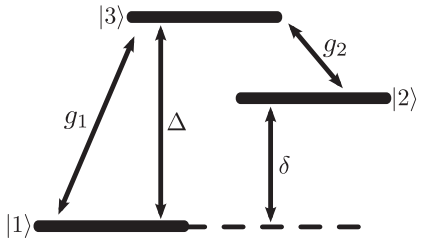

FIG. 1. Single-particle energy levels in Λ configuration: The excited state $|3\rangle$ is coupled via the two bosonic modes with frequencies ω_1 and ω_2 to either of the two ground states, $|1\rangle$ and $|2\rangle$, respectively. The corresponding coupling strengths are given by g_1 and g_2.

Dicke model [38]. The normal phase has zero occupation of the bosonic modes and all three-level systems occupy their respective single-particle ground-state $|1\rangle$. In contrast, the superradiant phases are characterized by a macroscopic occupation of the bosonic modes and the three-level systems. The superradiant phases are divided into a so-called blue and red superradiant phase. For the blue superradiant phase, the left branch of the Λ model is macroscopically occupied, whereas for the red superradiant phase it is the right branch that shows macroscopic occupation. The phase diagram features phase transitions of different order; the phase transition between the blue superradiant phase and the normal phase is continuous. In contrast, for finite δ, the phase transition between the normal and the red superradiant phase is of first order. Eventually, in the limit $\delta \to 0$ this phase transition becomes continuous as well. The two superradiant phases are separated by a first-order phase transition, irrespective of the parameters of the model.

B. Evaluation of the partition sum

All thermodynamic information of the equilibrium system is contained in the partition sum [67], $\mathcal{Z} = \mathcal{Z}(\mathcal{N},T) = \mathrm{Tr}\{\exp[-\beta\hat{H}]\}$. Here, T is the temperature and $\beta = 1/(k_\mathrm{B}T)$, with Boltzmann's constant k_B.

In order to evaluate the trace, we represent the bosonic degrees of freedom by coherent states [68,69] with respect to the $\hat{a}_n$ and the trace of the particle degrees of freedom are split into single-particle traces Tr_n,

$$\mathcal{Z} = \int_{\mathbb{C}} \frac{d^2\alpha_1}{\pi} \int_{\mathbb{C}} \frac{d^2\alpha_2}{\pi} \langle \alpha_1,\alpha_2 | \left(\prod_{n=1}^{\mathcal{N}} \mathrm{Tr}_n \right) e^{-\beta\hat{H}} |\alpha_1,\alpha_2\rangle . \quad (3)$$

Both integrals extend over the complex plane, respectively. Due to the coherent states, the bosonic part of the trace is easily computed. For the particle part of the trace, we observe that the $\mathcal{N}$ single-particle traces are all identical. In addition, we decompose both α_1 and α_2 in its real and imaginary part and scale them with $\sqrt{\mathcal{N}}$,

$$\alpha_n = \sqrt{\mathcal{N}}\, y_n + i\sqrt{\mathcal{N}}\, z_n, \quad n = 1,2. \quad (4)$$

Considering the thermodynamic limit $\mathcal{N} \to \infty$, the partition sum eventually reads

$$\mathcal{Z} = \frac{\mathcal{N}^2}{\pi^2} \int_{\mathbb{R}^4} dy_1 dz_1 dy_2 dz_2\, e^{-\beta\mathcal{N}\sum_{n=1}^{2} \hbar\omega_n (y_n^2+z_n^2)} \mathrm{Tr}\{e^{-\beta\hat{h}}\}^{\mathcal{N}}. \quad (5)$$

Here, the single-particle Hamiltonian $\hat{h} = \hat{h}(y_1,y_2)$ is given by

$$\hat{h}(y_1,y_2) = \delta\hat{a}_{2,2} + \Delta\hat{a}_{3,3} + 2g_1y_1(\hat{a}_{1,3}+\hat{a}_{3,1}) + 2g_2y_2(\hat{a}_{2,3}+\hat{a}_{3,2}). \quad (6)$$

Since all particles are identical, we have omitted the superindex k at the single-particle operators $\hat{a}^{(k)}_{n,m}$.

The remaining single-particle trace is evaluated in the eigenbasis of the single-particle Hamiltonian,

$$\hat{h} = \begin{pmatrix} 0 & 0 & 2g_1y_1 \\ 0 & \delta & 2g_2y_2 \\ 2g_1y_1 & 2g_2y_2 & \Delta \end{pmatrix}, \quad (7)$$

where we have chosen a convenient basis for the matrix representation of $\hat{a}_{n,m}$.

By virtue of Cardano's formula, the eigenvalues of $\hat{h}$ can be calculated exactly. However, the discussion of whether there is a phase transition or not and the analysis of the phase transition, is not very transparent. Therefore, we will pass the general case to a numerical computation and first consider the special case with $\delta = 0$ only, which is amenable to analytical calculations.

For $\delta = 0$, the partition sum can be written in compact form as (again in the thermodynamic limit $\mathcal{N} \to \infty$)

$$\mathcal{Z} = \frac{\mathcal{N}^2}{\pi^2} \int_{\mathbb{R}^2} dy_1 dz_1 \int_{\mathbb{R}^2} dy_2 dz_2\, e^{-\mathcal{N}f}, \quad (8)$$

with

$$f = f(y_1,y_2,z_1,z_2) = \beta\hbar\omega_1 y_1^2 + \beta\hbar\omega_2 y_2^2 + \beta\hbar\omega_1 z_1^2 + \beta\hbar\omega_2 z_2^2 - \ln\left[1 + 2e^{-\beta\Delta/2} \cosh\left(\frac{\beta\Delta}{2}\Omega\right)\right] \quad (9)$$

and a corresponding Ω given by

$$\Omega = \Omega(y_1,y_2) = \sqrt{1 + 16g_1^2y_1^2/\Delta^2 + 16g_2^2y_2^2/\Delta^2}. \quad (10)$$

The remaining integrals cannot be done exactly. However, we can approximate them for large $\mathcal{N}$ by Laplace's method [70]. Since large values of f are exponential suppressed, the main contribution to the integral is given by the global minimum of f. Given the minimum, the partition sum is proportional to

$$\mathcal{Z} \propto e^{-\mathcal{N}f_0}, \quad (11)$$

where $f_0 = f(y_{1,0},y_{2,0})$ with the position the minimum $(y_{1,0},y_{2,0})$. We anticipate that both z_n are identical zero at the minimum. This will be shown below. Hence, the leading contribution to the free energy F [67] is given by $F = \mathcal{N}k_\mathrm{B}Tf_0$.

Before we determine the minimum of f, we will first compute expectation values of observables using the same approximations as above.

C. Expectation values

In order to identify the phases and phase transitions, we discuss several observables. Of interest are the occupations of the bosonic modes, $\langle \hat{a}_m^\dagger \hat{a}_m \rangle$,$(m = 1,2)$, and the three-level systems, $\langle \hat{A}_n{}^n \rangle$,$(n = 1,2,3)$. In addition, the quantities $\langle \hat{A}_1{}^3 \rangle$ and $\langle \hat{A}_2{}^3 \rangle$ are considered. The real part of these give the macroscopic polarizations of the three-level systems of the

left and the right branch of the Λ model, respectively. They are generalizations of the polarization in the Dicke model. There, the polarization is proportional to the expectation value of the x component of the atomic pseudospin operator.

For functions G of operators of the two bosonic modes, the expectation value is given by (the calculation can be found in Appendix A1)

$$\langle G(\hat{a}_1^\dagger,\hat{a}_1,\hat{a}_2^\dagger,\hat{a}_2)\rangle = G(\sqrt{\mathcal{N}}\,y_{1,0},\sqrt{\mathcal{N}}\,y_{1,0},\sqrt{\mathcal{N}}\,y_{2,0},\sqrt{\mathcal{N}}\,y_{2,0}). \quad (12)$$

With that, we obtain for the occupation of both modes

$$\langle \hat{a}_n^\dagger \hat{a}_n\rangle = \mathcal{N}\,y_{n,0}^2. \quad (13)$$

Expectation values of collective operators of the three-level systems can be calculated in a similar manner. Let $\hat{M}$ be a collective operator and $\hat{m}^{(n)}$ the corresponding single-particle operator for the nth three-level system, such that

$$\hat{M} = \sum_{n=1}^{\mathcal{N}} \hat{m}^{(n)}. \quad (14)$$

Then, the mean value of $\hat{M}$ is given by (the calculation can be found in Appendix A2)

$$\langle \hat{M}\rangle = \mathcal{N}\,\langle \hat{m}\rangle_0\,. \quad (15)$$

Here, $\langle\cdot\rangle_0$ is the single-particle expectation value for a thermal state with the single-particle Hamiltonian $\hat{h}$ evaluated at the minimum $(y_{1,0},y_{2,0})$ of f. Thus, the expectation values for the collective atomic operators $\hat{A}_n^{\,m}$ can be traced back to the single-particle operators $\hat{a}_{n,m}$,

$$\left\langle \hat{A}_n^{\,m}\right\rangle = \mathcal{N}\,\langle \hat{a}_{n,m}\rangle_0\,. \quad (16)$$

This derivation and the following calculation holds even for nonzero δ.

Let ε_n be the eigenvalues and $\boldsymbol{w}_n$ the corresponding eigenvectors of $\hat{h}_0$. Then we evaluate the traces in Eq. (16) in this eigenbasis and the expectation values can be written as

$$\left\langle \hat{A}_n^{\,m}\right\rangle = \mathcal{N}\frac{1}{z}\sum_{k=1}^{3}(\boldsymbol{w}_k^*)_n(\boldsymbol{w}_k)_m\,e^{-\beta\varepsilon_k}. \quad (17)$$

Here $z = \mathrm{Tr}\{\exp[-\beta\hat{h}_0]\}$ is the partition sum of the single-particle Hamiltonian $\hat{h}_0$ and we have used that the matrix elements of $\hat{a}_{n,m}$ are given by zeros, except for the entry of the nth row and mth column, which is one.

D. Partition sum

We continue with the calculation of the partition sum, Eq. (8). Therefore, we need to find the minimum of f, Eq. (9). This analysis will be done in the following.

The variable z_n enters only quadratically in f, such that upon minimizing f, both z_n need to be zero. Minimizing f with respect to y_n yields the two equations ($n = 1,2$)

$$0 = y_n\left[\left(\frac{g_{n,c}}{g_n}\right)^2\Omega - q(\Omega)\right], \quad (18)$$

with

$$q(\Omega) = \frac{2e^{-\beta\Delta/2}\sinh\left[\frac{\beta\Delta}{2}\Omega\right]}{1+2e^{-\beta\Delta/2}\cosh\left[\frac{\beta\Delta}{2}\Omega\right]}, \quad (19)$$

and

$$g_{n,c} = \frac{\sqrt{\Delta\hbar\omega_n}}{2}. \quad (20)$$

Of course, Eqs. (18) are always solved by the trivial solution $y_1 = y_2 = 0$. But do nontrivial solutions exist, and for which parameter values?

We first observe that Eqs. (18) do not support solutions where both y_1 and y_2 are nonzero. For given y_1 and y_2, the parameter $\Omega = \Omega(y_1,y_2)$ is fixed. Then the squared bracket cannot be zero for both equations. Hence, the nontrivial solutions are given by one y_n being zero and the other being finite. In the following, the nonzero solution will be called $y_{n,0}$.

To check whether a nonzero $y_{n,0}$ really exists, we have to analyze the equation

$$0 = \left(\frac{g_{n,c}}{g_n}\right)^2\Omega_{n,0} - q(\Omega_{n,0}), \quad (21)$$

with

$$\Omega_{n,0} = \sqrt{1+4\frac{\hbar\omega_n}{\Delta}\left(\frac{g_n}{g_{n,c}}\right)^2 y_{n,0}^2}. \quad (22)$$

The function $q(\Omega)$ is bounded by one (see left panel of Fig. 2) and Ω itself is always greater or equal one. Therefore, for $g_n < g_{n,c}$, Eq. (21) has no solution and y_n has to be zero as well.

On the other hand, for $g_n > g_{n,c}$, nontrivial solutions of Eq. (21) can exist. In the right panel of Fig. 2, both terms of Eq. (21) are drawn. We see that for every finite temperature, the two curves always intersect twice, so that Eq. (21) always has two solutions. Of course, for a differentiable f, the two solutions cannot both correspond to minima of f. Hence, one solution stems from a maximum and the other from a minimum. Since the right side of Eq. (21) is the derivative of f, its sign-change signals whether a maximum (plus-minus sign change) or a minimum (minus-plus sign change) is passed

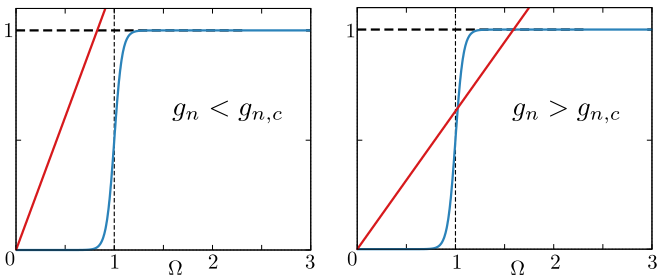

FIG. 2. Graphical analysis of Eq. (21) for $g_n < g_{n,c}$ (left) and $g_n > g_{n,c}$ (right) for a certain n and fixed temperature. The red straight line corresponds to the first term, $(\frac{g_{n,c}}{g_c})^2\Omega$, the other blue curved line corresponds to $q(\Omega)$ of Eq. (21) involving the hyperbolic functions. Of physical relevance is the region $\Omega > 1$ only. Thus, for $g < g_{n,c}$ no physical solution is possible, whereas for $g_n > g_{n,c}$ a physical solution might exist.

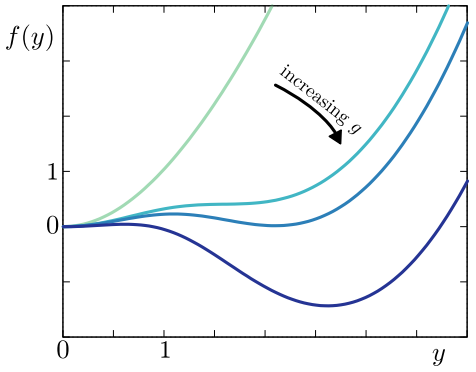

FIG. 3. The function f of Eq. (9) with $z_n = 0 = y_2$, and $y_1 = y$ for fixed temperature. The coupling strength g increases from the upper to the lower curves. The units are arbitrary and f has been rescaled for comparison, such that $f(0) = 0$ for all coupling strengths g. On increasing g, a local minimum forms distant from the origin. For large g this minimum eventually becomes a global minimum.

when Ω is increased. Therefore, the first solution corresponds to a maximum and the second to a minimum.

We gain additional insight, if we directly analyze $f(y_n)$ for different coupling strengths [$f(y_n) \equiv f(y_1,0,0,0)$ from Eq. (9), w.l.o.g. $n = 1$]. This is shown in Fig. 3. We see that for small coupling strengths, $f(y_n)$ has one local minimum only, which is located at $y_n = 0$, the trivial solution. If the coupling strength is increased, a maximum-minimum pair forms at finite values of y_n. In general, this local minimum at $y_n > 0$ is energetically higher than the local minimum of the trivial solution at $y_n = 0$, cf. Fig. 3. Hence, the trivial solution still minimizes $f(y_n)$ globally. However, if the coupling strength is increased even further, the local minimum at $y_n > 0$ becomes the global minimum. So we see that the position $y_{n,0}$ of the global minimum jumps at a certain value of the coupling strength from zero to a finite value.

The above discussion refers to the case $\delta = 0$. However, for finite δ, the results are qualitatively the same. We discuss the properties of the phase transition for finite δ below.

III. THE PHASE TRANSITION

In the above analysis, we have shown the existence of three different minima of f appearing in the exponent of the integrand of the partition sum. We have also shown that for a given temperature T, we find coupling strengths $g_{1,c}(T)$, $g_{2,c}(T)$, below which the trivial solution $y_{1,0} = y_{2,0} = 0$ minimizes f. In Eq. (13), $y_{n,0}$ measures the macroscopic occupation of the bosonic modes and can therefore serve as an order parameter of the phase transition. Hence, in the parameter regime where the trivial solution minimizes f, the system is in the normal phase.

In addition, above the coupling strengths $g_{1,c}(T)$, $g_{2,c}(T)$, f is minimized by nonzero values of either $y_{1,0}$ or $y_{2,0}$. The first corresponds to the red superradiant phase, the latter to the blue superradiant phase of Ref. [55]. The two superradiant phases at nonzero temperatures show only one macroscopically occupied bosonic mode as well; mode one for the blue superradiant phase and mode two for the red superradiant phase, while the occupation of the other mode is zero.

As we have seen in the previous section, the location of the global minimum $y_{n,0}$ jumps from the trivial solution to nonzero solutions. A jump of the order parameter defines a first-order phase transition. Therefore, the finite-temperature superradiant phase transition in the Λ model is a first-order phase transition. Hence, the continuous phase transition at zero temperature of Ref. [55] transforms into a first-order phase transition at finite temperatures.

So far, we have identified the phases and phase transitions using the occupation of the bosonic modes. In the following, we will further characterize the phases using observables of the three-level systems.

A. Normal phase

In the normal phase with $y_{1,0} = y_{2,0} = 0$, the Hamiltonian $\hat{h}_0$ is diagonal and the eigenvectors $\boldsymbol{w}_k$ are given by Cartesian unit vectors. Hence, the expectation value of all collective operators $\hat{A}_n^m$ with $n \neq m$ vanish. Conversely for the diagonal operators $\hat{A}_n^n$, the occupations; their expectation values are given by

$$\langle \hat{A}_1^1 \rangle = \mathcal{N} \frac{1}{1 + e^{-\beta\delta} + e^{-\beta\Delta}}, \tag{23}$$

$$\langle \hat{A}_2^2 \rangle = \mathcal{N} \frac{e^{-\beta\delta}}{1 + e^{-\beta\delta} + e^{-\beta\Delta}}, \tag{24}$$

and

$$\langle \hat{A}_3^3 \rangle = \mathcal{N} \frac{e^{-\beta\Delta}}{1 + e^{-\beta\delta} + e^{-\beta\Delta}}. \tag{25}$$

Here, we explicitly see that in the normal phase the expectation values are independent of the coupling strengths g_1 and g_2. Furthermore, we note that for finite temperatures, in addition to the single-particle ground state $|1\rangle$, the energetically higher-lying single-particle states $|2\rangle$ and $|3\rangle$ are macroscopically excited as well. Hence, in contrast to the bosonic modes, the particle part of the system gets thermally excited. From that point of view, i.e., concerning the populations of the single-particle energy levels, the particle system in the normal phase behaves like a *normal* thermodynamical system.

B. Superradiant phases

For the superradiant phases, we cannot give explicit expressions for the expectation values, neither for finite or vanishing δ. That is because we need to compute the minimum of f numerically. Though for $\delta = 0$, we can say that some expectation values are exactly zero. This will be done next, separately for the red and the blue superradiant phases.

1. Red superradiant phase

First consider the red superradiant phase with $y_{1,0} \equiv y_0 \neq 0$ and $y_{2,0} = 0$. Then, the single-particle Hamiltonian $\hat{h}(y_0,0)$ reads [cf. Eq. (7)]

$$\hat{h}(y_0,0) = \begin{pmatrix} 0 & 0 & 2g_1 y_0 \\ 0 & 0 & 0 \\ 2g_1 y_1 & 0 & \Delta \end{pmatrix}, \tag{26}$$

and its exponential has the form

$$e^{-\beta\hat{h}(y_0,0)} = \begin{pmatrix} a_+ & 0 & b_1 \\ 0 & 1 & 0 \\ b_1 & 0 & a_- \end{pmatrix}. \tag{27}$$

The matrix elements $a_\pm$ and b_n are given by (the matrix element b_2 is needed below).

$$a_\pm = e^{-\frac{\beta\Delta}{2}} \left(\cosh\left[\frac{\beta\Delta\Omega}{2}\right] \pm \frac{\sinh\left[\frac{\beta\Delta\Omega}{2}\right]}{\Omega} \right), \tag{28}$$

$$b_n = -\frac{4g_n y_n}{\Delta\Omega} e^{-\frac{\beta\Delta}{2}} \sinh\left[\frac{\beta\Delta\Omega}{2}\right], \quad n = (1,2). \tag{29}$$

The product of the exponential operator, Eq. (27), with matrices of the form

$$\begin{pmatrix} 0 & M_{12} & 0 \\ M_{21} & 0 & M_{23} \\ 0 & M_{32} & 0 \end{pmatrix} \tag{30}$$

is traceless. Therefore, the expectation values of the collective operators $\hat{A}_1^{\,2}$, $\hat{A}_2^{\,3}$ and their Hermitian conjugates are zero, i.e., there is no spontaneous polarization between both the single-particle states $|1\rangle$ and $|2\rangle$, and the single-particle states $|2\rangle$ and $|3\rangle$. Contrary, the polarization in the left branch of the Λ model, i.e., between the states $|1\rangle$ and $|3\rangle$, is finite and macroscopic.

2. *Blue superradiant phase*

For the blue superradiant case, the discussion is similar. Here we have $y_{2,0} \equiv y_0 \neq 0$ and $y_{1,0} = 0$, and the exponential of the single-particle Hamiltonian reads

$$e^{-\beta\hat{h}(0,y_0)} = \begin{pmatrix} 1 & 0 & 0 \\ 0 & a_+ & b_2 \\ 0 & b_2 & a_- \end{pmatrix}. \tag{31}$$

The matrix elements are given above, Eqs. (28) and (29). Now, the product of the exponential operator, Eq. (31), with matrices of the form

$$\begin{pmatrix} 0 & M_{12} & M_{13} \\ M_{21} & 0 & 0 \\ M_{31} & 0 & 0 \end{pmatrix} \tag{32}$$

is traceless and thus expectation values of the collective operators $\hat{A}_1^{\,2}$, $\hat{A}_1^{\,3}$ and their Hermitian conjugates are zero. On the other hand, the expectation value of the operators $\hat{A}_2^{\,3}$, $\hat{A}_3^{\,2}$ is finite and macroscopic. Hence, only the transition in the right branch of the Λ model is spontaneously polarized.

In conclusion, we find that in the superradiant phases at finite temperature, only the corresponding branch of the Λ model shows spontaneous polarization: the left branch in the red superradiant phase and the right branch in the blue superradiant phase. In the normal phase, the polarization is completely absent. Hence, in contrast to the populations of the atomic system, the polarizations are not thermally excited and show a genuine quantum character. Thus, both the polarizations and the occupations of the two resonator modes show a similar behavior in the three phases. Therefore, we have two sets of observables, the polarizations for the three-level systems and the occupations of the bosonic modes, to detect the superradiant phase transition at finite temperatures.

C. Numerical evaluation of the partition sum

The above analysis for vanishing δ already shows that the phase transition in the Λ model for finite temperatures is a first-order phase transition. This fact renders the calculation of the exact location of the phase transition with our methods impossible. This can be understood with the help of the free energy as follows. In the thermodynamic limit, the global minimum of the free energy defines the thermodynamic phase of the system. We explicitly saw this when we have computed the partition sum. In a phase transition, the system changes from one thermodynamic state to another thermodynamic state. This new state corresponds to a different, now global minimum of the free energy.

For continuous phase transitions, the new minimum evolves continuously from the first minimum and the first minimum changes its character to a maximum. Hence, the continuous phase transition is characterized by a sign-change of the curvature of the free energy at the position of the minimum of the state describing the normal phase. Often, this is tractable analytically.

In contrast in the case of first-order phase transitions, the new global minimum of the free energy appears distant from the old global minimum of the free energy, cf. Fig. 3. There are still two minima and we cannot detect the phase transition by the curvature of the free energy. Thus, to find the phase transition for first-order phase transitions, we first need to find all minima of the free energy and then find the global minima of these. This has to be done numerically here.

For the numerical computation, we do not solve Eq. (18), but we test for the minima of $f(y_1,y_2)$, Eq. (9), directly. Therefore, we apply a brute-force method, i.e., we look for the smallest value of $f(y_1,y_2)$ on a y_1-y_2 grid. Due to the reflection symmetry of $f(y_1,y_2)$, we can confine the grid to positive values for y_1 and y_2. This yields the position of the minimum $(y_{1,0},y_{2,0})$. Then we compute the eigenvalues and eigenvectors of the Hamiltonian $\hat{h}$ at this point and obtain via Eq. (A1) the expectation values for the operators of the bosonic modes, and via Eq. (17) the corresponding expectation values for the three-level systems.

Figures 4, 5, and 6 show the occupation $\langle \hat{a}_n^\dagger \hat{a}_n \rangle$ of the modes of the resonator, the occupation $\hat{A}_n^{\,n}$ of the single-particle levels of the atoms, and the polarizations $\hat{A}_1^{\,3}$, $\hat{A}_2^{\,3}$ of the atoms for low and high temperatures, respectively. All plots have been generated numerically for finite values of δ.

These figures corroborate our findings from the analytical discussion of the partition sum for vanishing δ. We see three phases: a *normal* phase for coupling strengths g_1 and g_2 below the critical coupling strengths $g_{1,c}$ and $g_{2,c}$, a *red superradiant* phase for large coupling strengths g_1 above the critical coupling strength $g_{1,c}$, and a *blue superradiant* phase for coupling strengths g_2 above the critical coupling strength $g_{2,c}$.

The normal phase is characterized by a zero occupation of both bosonic modes (Fig. 4) In addition, the polarization, or coherence, of the three-level systems is zero in the normal phase (Fig. 6).

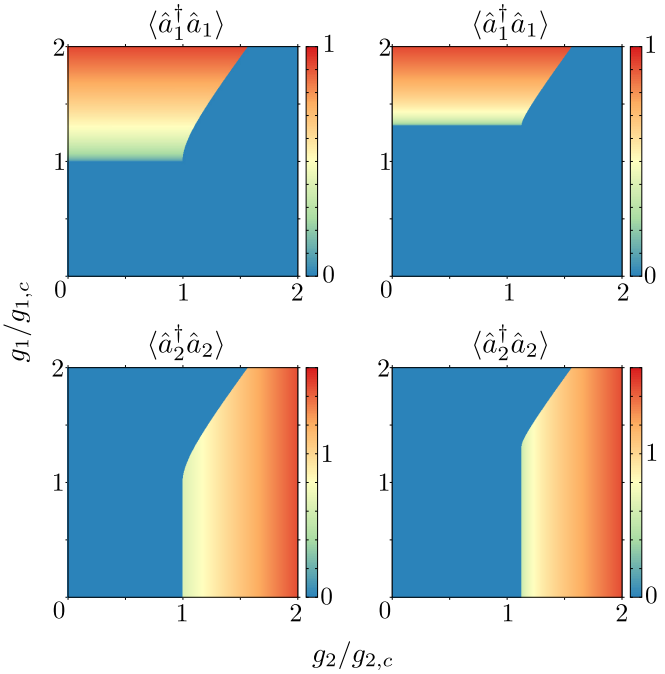

FIG. 4. Numerical computation of the scaled occupations $\langle \hat{a}_n^\dagger \hat{a}_n \rangle / \mathcal{N}$ of the two bosonic modes for $k_B T = 0.001\,\Delta$ (left) and $k_B T = 0.25\,\Delta$ (right). The parameters are set to $\Delta = 1$, $\delta = 0.1$, $\omega_1 = 1.1$, and $\omega_2 = 0.8$. The computation has been done in the thermodynamic limit using Laplace's method.

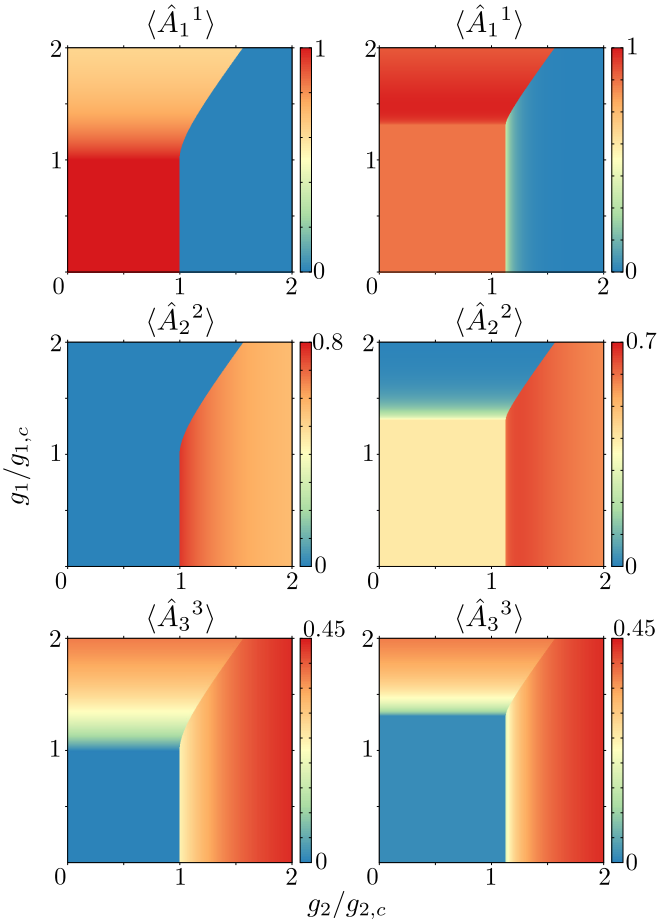

FIG. 5. Numerical computation of the scaled occupations $\langle \hat{A}_n{}^n \rangle / \mathcal{N}$ of the single-particle energy levels of the three-level systems for $k_B T = 0.001\,\Delta$ (left) and $k_B T = 0.25\,\Delta$ (right). Parameters as in Fig. 4.

In contrast to the normal phase, the two superradiant phases are characterized by a macroscopic occupation of only one of the two bosonic modes: mode one in the red superradiant phase and mode two in the blue superradiant phase. In addition, the red (blue) superradiant phase shows a spontaneous polarization $\langle \hat{A}_1{}^3 \rangle$ ($\langle \hat{A}_2{}^3 \rangle$).

We see that these defining properties remain for increasing temperature (right part of Figs. 4–6). As discussed in Sec. III A, we see that the population $\langle \hat{A}_2{}^2 \rangle$ of the single-particle energy level $|2\rangle$ increases for rising temperature. The same is true for the occupation $\langle \hat{A}_3{}^3 \rangle$, though this is not visible in the right part of Fig. 5 due to the fact that the temperature is yet too small.

From the Figs. 4–6 we also see that the shape of the phase boundary remains a straight line between the normal and the two superradiant phases. Between the red and the blue superradiant phases, the form of the phase boundary seems to persist as well. The only effect of the rising temperature is a shift of the phase boundary toward higher values of the coupling strengths g_1 and g_2. This is visualized in Fig. 7 where the polarization $\langle \hat{A}_1{}^3 \rangle$ of the transition $|1\rangle \leftrightarrow |3\rangle$ of the three-level systems is shown for variable coupling strength g_1 and temperature T. The coupling strength of the second mode is fixed to $g_2 = 0.2\, g_{2,c}$. We see that for increasing temperature, the superradiant phase diminishes.

In addition to the shift of the phase boundary, the jump in the observables at this first-order phase transition increases. This is shown in Fig. 8 for the occupation $\langle \hat{a}_1^\dagger \hat{a}_1 \rangle$ of the first bosonic mode. Of course, numerically, jumps are hard to detect since we get a discrete set of points as an output anyway. However, the dotted lines in Fig. 8 connect two largely separated points;

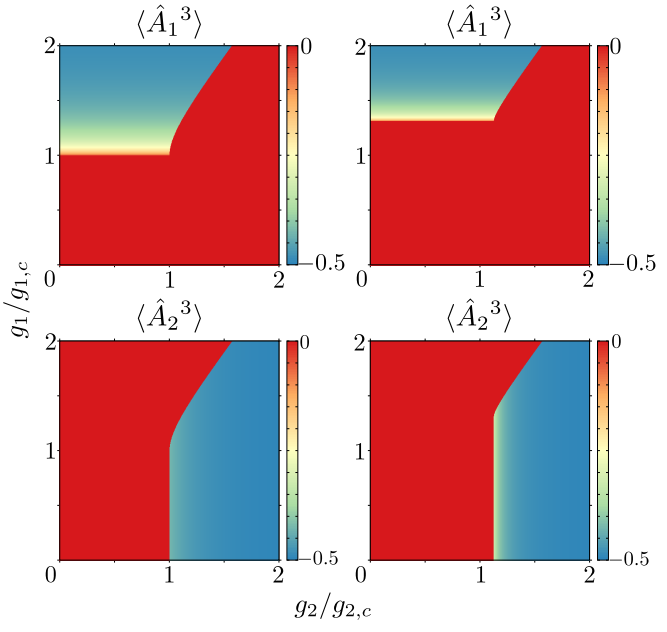

FIG. 6. Numerical computation of the scaled polarizations $\langle \hat{A}_1{}^3 \rangle / \mathcal{N}$, $\langle \hat{A}_2{}^3 \rangle / \mathcal{N}$ of the three-level systems for $k_B T = 0.001\,\Delta$ (left) and $k_B T = 0.25\,\Delta$ (right). Parameters as in Fig. 4.

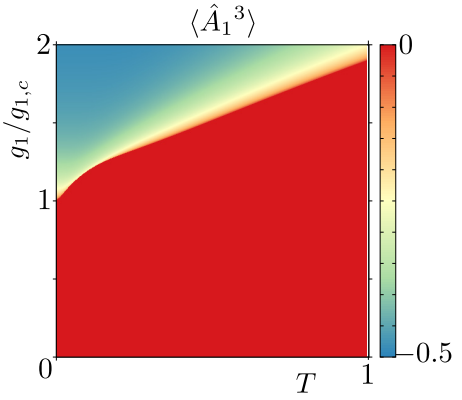

FIG. 7. Numerical computation of the scaled polarization $\langle \hat{A}_1{}^3 \rangle / \mathcal{N}$ of the transition $|1\rangle \leftrightarrow |3\rangle$ of the three-level system. Parameters as in Fig. 4 and $g_2 = 0.2\, g_{2,c}$.

each of the lines consists of 1000 data points. Thus, we can really speak of jumps in the observables and thus of a first-order phase transition.

D. Zero-temperature limit

Last, we analyze the zero-temperature limit of the Λ model for $\delta = 0$. For decreasing temperature, the function $q(\Omega)$, Eq. (19), becomes more and more step function like. Indeed, for $\beta\Delta \gg 1$, $q(\Omega)$ can be written as a Fermi function, and eventually in the limit $\beta\Delta \to \infty$, $q(\Omega)$ is given by

$$q(\Omega) = \begin{cases} 0, & \Omega < 1 \\ 1, & \Omega > 1. \end{cases} \tag{33}$$

Hence, at zero temperature, Eq. (21) has always a unique solution for coupling strengths $g_n > g_{n,c}$. In addition, since $f(y)$ shows no additional maximum, we have a continuous phase transition in this quantum limit.

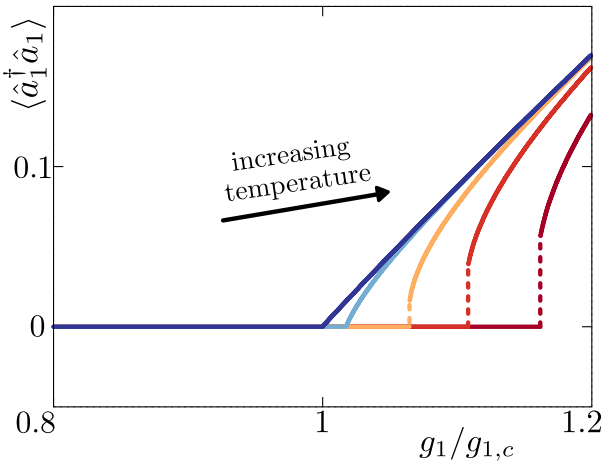

FIG. 8. Occupations $\langle \hat{a}_1^\dagger \hat{a}_1 \rangle$ of the first bosonic mode as a function of the coupling strength g_1 for fixed coupling strength $g_2 = 0.2 g_{2,c}$ and rising temperature (left to right, blue to red, respectively). The other parameters are set to $\Delta = 1$, $\delta = 0.1$, $\omega_1 = 1.1$, and $\omega_2 = 0.8$.

Furthermore, we can also compute the position of the minimum of f. In the limit $T \to 0$, Eq. (21) reads

$$0 = \left(\frac{g_{n,c}}{g_n}\right)^2 \sqrt{1 + \frac{4\hbar\omega_n}{\Delta}\left(\frac{g_n}{g_{n,c}}\right)^2 y_n^2} - 1. \tag{34}$$

Solving for y_n, we obtain

$$y_n = \pm \frac{g}{\hbar\omega_n} \sqrt{1 - \left(\frac{g_{n,c}}{g_n}\right)^4}. \tag{35}$$

If we identify y_n with the mean fields φ_n of Ref. [55], we reproduce our results [55] for the superradiant phases of the quantum phase transition of the Λ model.

The mean fields Ψ_n of Ref. [55] can be reproduced as well. Consider for instance Ψ_3, which is related to $\langle \hat{A}_3{}^3 \rangle$ through $\langle \hat{A}_3{}^3 \rangle = \mathcal{N}\Psi_3^2$, except for a possible phase. Using the results for the Boltzmann operator in the red superradiant phase, Eq. (31), plus the above expression for y_1, Eq. (35), and finally insert everything into the expectation value of Eq. (16), we obtain

$$\langle \hat{A}_3{}^3 \rangle = \frac{\mathcal{N}}{2} \frac{1 - e^{\beta\Delta\Omega} + (1 + e^{\beta\Delta\Omega})\Omega}{[1 + e^{\beta\Delta\Omega} + e^{\frac{\beta\Delta}{2}(\Omega+1)}]\Omega}, \tag{36}$$

which in the zero-temperature limit $\beta\Delta \to \infty$ reduces to

$$\langle \hat{A}_3{}^3 \rangle = \frac{\mathcal{N}}{2} \frac{\Omega - 1}{\Omega}. \tag{37}$$

Here, $\Omega = \Omega(y_1)$ from Eq. (22). If we finally insert the position y_1 of the minimum of the free energy, Eq. (35), the population of the third single-particle energy level in the zero-temperature limit is given by

$$\langle \hat{A}_3{}^3 \rangle = \frac{\mathcal{N}}{2}\left[1 - \left(\frac{g_{1,c}}{g_1}\right)^2\right], \tag{38}$$

which agrees with the findings of Ref. [55] for Ψ_3. Applying the same technique, we can obtain the expectation values of all other collective atomic operators $\hat{A}_n{}^m$ in both superradiant phases. This again coincides with the results of Ref. [55].

IV. CONCLUSION

We have analyzed the Λ model in the thermodynamic limit at finite temperatures using the partition sum of the Hamiltonian. Compared to the quantum phase transition of this model [55], we found that at finite temperatures the properties of the phases and phase transition partially persist. Namely, we found three phases: a normal and two superradiant phases. These have the same properties as in the quantum limit. For small couplings and/or at high temperatures, the system is in the normal phase, where all particles are in their respective single-particle ground-state and both bosonic modes are in their vacuum state. If one of the coupling strengths is increased above a temperature-dependent critical coupling strength, the system undergoes a phase transition into a superradiant phase, which is characterized by a macroscopic occupation of one of the bosonic modes only and a spontaneous polarization of the corresponding branch of the three-level system.

A new characteristic of the phase transition at finite temperatures is the appearance of first-order phase transitions only.

For the quantum phase transition we already found first-order phase transitions between the normal and the red superradiant phase and between the two superradiant phases. Here, at finite temperatures, the phase transition from the normal to the blue superradiant phase becomes a first-order phase transition as well. This change of the order of the phase transition would appear for a single bosonic mode as well. Hence, it is due to the additional single-particle energy level that first-order phase transitions show up. In addition, we emphasise that even in the degenerate limit, $\delta \to 0$, the phase transitions from the normal to both superradiant phases are of first order.

It is remarkable that in contrast to the original Dicke model, the mean-field phase transitions at finite temperatures are not continuous. This facet becomes significant if *real* atoms and photons are considered. Here, for the original Dicke model with its continuous phase transition, there exists a no-go theorem [36,57–63]. However, for first-order mean-field quantum phase transitions, it is known [56,66] that this no-go theorem does not apply and superradiant phase transitions occur. We expect an identical conclusion for the Λ model at finite temperatures.

The effect of finite temperature is relevant for an experimental realization as well. In fact, the original Dicke model has been implemented via an effective Hamiltonian in experiment [3,4,6,7,9]. By an extension of the experimental setup (inclusion of additional energy levels and modes and cavity modes) it should be possible to realize an effective description of our extended Dicke model and observe this first-order superradiant phase transition.

ACKNOWLEDGMENTS

This work was supported by the Deutsche Forschungsgemeinschaft within the SFB 910, the GRK 1558, and the projects BR 1528/82 and 1528/9.

APPENDIX

1. Expectation values of bosonic mode operators

We calculate the expectation value of functions G of operators of the two bosonic modes as

$$\langle G(\hat{a}_1^\dagger,\hat{a}_1,\hat{a}_2^\dagger,\hat{a}_2)\rangle = \frac{1}{\mathcal{Z}}\mathrm{Tr}\left\{G(\hat{a}_1^\dagger,\hat{a}_1,\hat{a}_2^\dagger,\hat{a}_2)\, e^{-\beta\hat{H}}\right\} \tag{A1}$$

$$= \frac{1}{\mathcal{Z}}\int_{\mathbb{C}^2}\frac{d^2\alpha_1 d^2\alpha_2}{\pi^2} G(\alpha_1^*,\alpha_1,\alpha_2^*,\alpha_2)\, e^{-\beta\sum_{n=1}^2\hbar\omega_n|\alpha_n|^2}\mathrm{Tr}\{e^{-\beta\hat{h}}\}^{\mathcal{N}} \tag{A2}$$

$$= \frac{1}{\mathcal{Z}}\frac{\mathcal{N}^2}{\pi^2}\int_{\mathbb{R}^2} dy_1 dy_2 G(\sqrt{\mathcal{N}}y_1,\sqrt{\mathcal{N}}y_1,\sqrt{\mathcal{N}}y_2,\sqrt{\mathcal{N}}y_2)\, e^{-\beta f} \tag{A3}$$

$$= G(\sqrt{\mathcal{N}}\,y_{1,0},\sqrt{\mathcal{N}}\,y_{1,0},\sqrt{\mathcal{N}}\,y_{2,0},\sqrt{\mathcal{N}}\,y_{2,0}). \tag{A4}$$

In the last step we used that the exponential dominates for large $\mathcal{N}$. Hence, the function G can be considered constant and the remaining integral plus the prefactor is equal to the partition sum.

2. Expectation values of operators of the three-level systems

For mean values of collective operators $\hat{M}$ (cf. Sec. II C) of the three-level systems we have

$$\langle\hat{M}\rangle = \frac{1}{\mathcal{Z}}\mathrm{Tr}\{\hat{M}e^{-\beta\hat{H}}\} \tag{A5}$$

$$= \frac{1}{\mathcal{Z}}\int_{\mathbb{C}^2}\frac{d^2\alpha_1 d^2\alpha_2}{\pi^2} e^{-\beta\sum_{n=1}^2\hbar\omega_n|\alpha_n|^2}\sum_{k=1}^{\mathcal{N}}\mathrm{Tr}\left\{\hat{m}^{(k)}e^{-\beta\hat{h}^{(1)}}\cdot\ldots\cdot e^{-\beta\hat{h}^{(\mathcal{N})}}\right\} \tag{A6}$$

$$= \frac{1}{\mathcal{Z}}\int_{\mathbb{C}^2}\frac{d^2\alpha_1 d^2\alpha_2}{\pi^2} e^{-\beta\sum_{n=1}^2\hbar\omega_n|\alpha_n|^2}\mathrm{Tr}\{e^{-\beta\hat{h}}\}^{\mathcal{N}}\mathcal{N}\frac{\mathrm{Tr}\{\hat{m}e^{-\beta\hat{h}}\}}{\mathrm{Tr}\{e^{-\beta\hat{h}}\}} \tag{A7}$$

$$= \mathcal{N}\frac{\mathrm{Tr}\{\hat{m}\, e^{-\beta\hat{h}_0}\}}{\mathrm{Tr}\{e^{-\beta\hat{h}_0}\}} \tag{A8}$$

$$\equiv \mathcal{N}\,\langle\hat{m}\rangle_0\,, \tag{A9}$$

with $\hat{h}_0 = \hat{h}(y_{1,0}, y_{2,0})$.

[1] R. H. Dicke, Phys. Rev. **93**, 99 (1954).
[2] K. Hepp and E. H. Lieb, Ann. Phys. **76**, 360 (1973).
[3] K. Baumann, C. Guerlin, F. Brennecke, and T. Esslinger, Nature (London) **464**, 1301 (2010).
[4] K. Baumann, R. Mottl, F. Brennecke, and T. Esslinger, Phys. Rev. Lett. **107**, 140402 (2011).
[5] H. Ritsch, P. Domokos, F. Brennecke, and T. Esslinger, Rev. Mod. Phys. **85**, 553 (2013).
[6] C. Hamner, C. Qu, Y. Zhang, J. Chang, M. Gong, C. Zhang, and P. Engels, Nat. Commun. **5**, 4023 (2014).
[7] J. Klinder, H. Keßler, M. R. Bakhtiari, M. Thorwart, and A. Hemmerich, Phys. Rev. Lett. **115**, 230403 (2015).
[8] F. Dimer, B. Estienne, A. S. Parkins, and H. J. Carmichael, Phys. Rev. A **75**, 013804 (2007).
[9] M. P. Baden, K. J. Arnold, A. L. Grimsmo, S. Parkins, and M. D. Barrett, Phys. Rev. Lett. **113**, 020408 (2014).
[10] J. Keeling, M. J. Bhaseen, and B. D. Simons, Phys. Rev. Lett. **105**, 043001 (2010).
[11] D. Nagy, G. Szirmai, and P. Domokos, Phys. Rev. A **84**, 043637 (2011).
[12] B. Öztop, M. Bordyuh, O. E. Müstecaplioglu, and H. E. Türeci, New J. Phys. **14**, 085011 (2012).
[13] M. J. Bhaseen, J. Mayoh, B. D. Simons, and J. Keeling, Phys. Rev. A **85**, 013817 (2012).
[14] G. Kónya, D. Nagy, G. Szirmai, and P. Domokos, Phys. Rev. A **86**, 013641 (2012).
[15] Emanuele G. Dalla Torre, S. Diehl, M. D. Lukin, S. Sachdev, and P. Strack, Phys. Rev. A **87**, 023831 (2013).
[16] W. Kopylov, C. Emary, and T. Brandes, Phys. Rev. A **87**, 043840 (2013).
[17] S. Genway, W. Li, C. Ates, B. P. Lanyon, and I. Lesanovsky, Phys. Rev. Lett. **112**, 023603 (2014).
[18] E. G. Dalla Torre, Y. Shchadilova, E. Y. Wilner, M. D. Lukin, and E. Demler, Phys. Rev. A **94**, 061802(R) (2016).
[19] J. Gelhausen, M. Buchhold, and P. Strack, arXiv:1605.07637.
[20] G. Konya, G. Szirmai, and P. Domokos, Eur. Phys. J. D **65**, 33 (2011).
[21] F. Piazza, P. Strack, and W. Zwerger, Ann. Phys. **339**, 135 (2013).
[22] P. Strack and S. Sachdev, Phys. Rev. Lett. **107**, 277202 (2011).
[23] J.-i. Inoue, J. Phys. A: Math. Theoret. **45**, 305003 (2012).
[24] H. Goto and K. Ichimura, Phys. Rev. A **77**, 053811 (2008).
[25] O. Tsyplyatyev and D. Loss, Phys. Rev. A **80**, 023803 (2009).
[26] J. Vidal and S. Dusuel, Europhys. Lett. **74**, 817 (2006).
[27] G. Liberti, F. Plastina, and F. Piperno, Phys. Rev. A **74**, 022324 (2006).
[28] L. Bakemeier, A. Alvermann, and H. Fehske, Phys. Rev. A **85**, 043821 (2012).
[29] V. M. Bastidas, C. Emary, B. Regler, and T. Brandes, Phys. Rev. Lett. **108**, 043003 (2012).
[30] G. Francica, S. Montangero, M. Paternostro, and F. Plastina, arXiv:1608.05049.
[31] T. Brandes, Phys. Rev. E **88**, 032133 (2013).
[32] Y. Yi-Xiang, J. Ye, and W.-M. Liu, Sci. Rep. **3**, 3476 (2013).
[33] A. Baksic and C. Ciuti, Phys. Rev. Lett. **112**, 173601 (2014).
[34] A. L. Grimsmo, A. S. Parkins, and B.-S. Skagerstam, New J. Phys. **16**, 065004 (2014).
[35] W. Kopylov, C. Emary, E. Schöll, and T. Brandes, New J. Phys. **17**, 013040 (2015).
[36] P. Nataf and C. Ciuti, Nat. Commun. **1**, 72 (2010).
[37] P. Nataf and C. Ciuti, Phys. Rev. Lett. **104**, 023601 (2010).
[38] C. Emary and T. Brandes, Phys. Rev. E **67**, 066203 (2003).
[39] C. Emary and T. Brandes, Phys. Rev. Lett. **90**, 044101 (2003).
[40] Y. K. Wang and F. T. Hioe, Phys. Rev. A **7**, 831 (1973).
[41] K. Hepp and E. H. Lieb, Phys. Rev. A **8**, 2517 (1973).
[42] H. J. Carmichael, C. W. Gardiner, and D. F. Walls, Phys. Lett. A **46**, 47 (1973).
[43] T. Brandes, Phys. Rep. **408**, 315 (2005).
[44] F. N. C. Paraan and A. Silva, Phys. Rev. E **80**, 061130 (2009).
[45] L. Fusco, M. Paternostro, and G. De Chiara, Phys. Rev. E **94**, 052122 (2016).
[46] P. Pérez-Fernández, P. Cejnar, J. M. Arias, J. Dukelsky, J. E. García-Ramos, and A. Relaño, Phys. Rev. A **83**, 033802 (2011).
[47] P. Pérez-Fernández, A. Relaño, J. M. Arias, P. Cejnar, J. Dukelsky, and J. E. García-Ramos, Phys. Rev. E **83**, 046208 (2011).
[48] R. Puebla, A. Relaño, and J. Retamosa, Phys. Rev. A **87**, 023819 (2013).
[49] R. Puebla and A. Relaño, Europhys. Lett. **104**, 50007 (2013).
[50] M. A. Bastarrachea-Magnani, S. Lerma-Hernández, and J. G. Hirsch, Phys. Rev. A **89**, 032101 (2014).
[51] M. A. Bastarrachea-Magnani, B. López-del Carpio, S. Lerma-Hernández, and J. G. Hirsch, Phys. Scr. **90**, 068015 (2015).
[52] C. M. Lóbez and A. Relaño, Phys. Rev. E **94**, 012140 (2016).
[53] M. A. Bastarrachea-Magnani, S. Lerma-Hernández, and J. G. Hirsch, J. Stat. Mech. (2016) 093105.
[54] M. Kloc, P. Stransky, and P. Cejnar, arXiv:1609.02758.
[55] M. Hayn, C. Emary, and T. Brandes, Phys. Rev. A **84**, 053856 (2011).
[56] M. Hayn, C. Emary, and T. Brandes, Phys. Rev. A **86**, 063822 (2012).
[57] K. Rzażewski, K. Wódkiewicz, and W. Żakowicz, Phys. Rev. Lett. **35**, 432 (1975).
[58] K. Rzażewski, K. Wódkiewicz, and W. Żakowicz, Phys. Lett. A **58**, 211 (1976).
[59] K. Rzażewski and K. Wódkiewicz, Phys. Rev. A **13**, 1967 (1976).
[60] J. M. Knight, Y. Aharonov, and G. T. C. Hsieh, Phys. Rev. A **17**, 1454 (1978).
[61] I. Bialynicki-Birula and K. Rzążnewski, Phys. Rev. A **19**, 301 (1979).
[62] V. A. Slyusarev and R. P. Yankelevich, Theor. Math. Phys. **40**, 641 (1979).
[63] O. Viehmann, J. von Delft, and F. Marquardt, Phys. Rev. Lett. **107**, 113602 (2011).
[64] C. Ciuti and P. Nataf, Phys. Rev. Lett. **109**, 179301 (2012).
[65] O. Viehmann, J. von Delft, and F. Marquardt, arXiv:1202.2916.
[66] A. Baksic, P. Nataf, and C. Ciuti, Phys. Rev. A **87**, 023813 (2013).
[67] R. P. Feynman, *Statistical Mechanics—A Set of Lectures*, Frontiers in Physics (W. A. Benjamin, Inc., Reading, MA, 1972).
[68] R. J. Glauber, Phys. Rev. **131**, 2766 (1963).
[69] F. T. Arecchi, E. Courtens, R. Gilmore, and H. Thomas, Phys. Rev. A **6**, 2211 (1972).
[70] C. M. Bender and S. A. Orszag, *Advanced Mathematical Methods for Scientists and Engineers* (Springer, New York, 1999).